# Electron–Electron Double Resonance of Free Radicals in Solution

JAMES S. HYDE
*Varian Associates, Analytical Instrument Division, Palo Alto, California*
JAMES C. W. CHIEN
*Hercules Research Center, Wilmington, Delaware*
AND
JACK H. FREED*
*Department of Chemistry, Cornell University, Ithaca, New York*†

(Received 23 October 1967)

The technique of electron–electron double resonance, in which one part of the EPR spectrum of a paramagnetic sample is irradiated with an intense microwave field and the effect of this intense field on other parts of the spectrum is determined utilizing a second weak microwave field, has been applied to free radicals in solution. EPR signals detected by the weak microwave source are *reduced* in intensity when the two frequencies are separated by an integral number of hyperfine intervals. In some cases this reduction is as much as 40%. A bimodal cavity of novel design capable of supporting the two resonant microwave modes is described. A nitroxide radical has been investigated in greatest detail. Two mechanisms have been identified: rapid nuclear relaxation induced by electron–nuclear dipolar (END) interaction, which is dominant at low concentrations and temperatures, and Heisenberg exchange (HE), dominant at high concentrations and temperatures. A theoretical analysis of the relaxation processes is presented which permits extracting the critical relaxation parameters from the experimental data. The main theme of the paper is a description of the basic effects, but there would appear to be a number of analytical or structural applications of this technique.

## I. INTRODUCTION

Double resonance involves the irradiation of a sample by electromagnetic energy at two frequencies. Electronic apparatus is designed such that each frequency must correspond to an interval in the energy-level diagram if a signal is to be detected. Experiments of this type are useful in the study of relaxation phenomena. In addition, this more restrictive condition for the observation of signals is of great help in the interpretation of complex spectra. Double resonance often is viewed as a technique for improving the effective resolution in spectroscopy.

In this paper we investigate electron–electron double resonance in which a free radical in solution is irradiated simultaneously by two microwave frequencies differing in energy by an amount equal to the separation of two of the hyperfine lines. After the two microwave frequencies have been preset by proper adjustment of the two klystrons and the bimodal sample cavity has been tuned to these two frequencies, the magnetic field is swept. This particular experiment differs somewhat from most other double resonance techniques in that two intervals are involved which do not have a common energy level.

Large electron–electron double resonance signals are seen in free radicals in solution under proper conditions, amounting in some cases to changes in EPR signal intensities of 40%. In this paper we describe the nature of these effects on several different free radicals under various conditions of temperature, concentration, and the two microwave power levels, and we propose theoretical explanations which appear consistent with the experimental results. During the course of these experiments several analytical applications have occurred to us, and some of these we intend to investigate in the future. Our main concern here is the study of relaxation processes governing this type of double resonance.

We are aware of three previous experiments of this general class, each concerned with defects in crystals and performed at liquid-helium temperatures.[1–3] Sorokin, Lasher, and Gelles[1] studied cross relaxation on nitrogen centers in diamond. They investigated an intermolecular or interdefect mechanism observable at relatively high concentrations. Unruh and Culvahouse[2] studied relaxation processes by irradiating the various hyperfine lines of $^{59}Co$ ($I=\frac{7}{2}$) introduced as an impurity into $La_2Zn_3(NO_3)_{12}\cdot 24H_2O$. Moran[3] studied the diffusion of energy through the inhomogeneously broadened $F$-center line in alkali halides.

The design of a bimodal microwave cavity which may be used to irradiate a sample simultaneously at two different microwave frequencies is a critical aspect of the experiment. The cavity employed here differs from others described in the literature and offers several advantages. In the second section of the paper, the cavity and other key aspects of the instrumentation are discussed.

The experiments and some of the spectra are pre-

* Alfred P. Sloan Foundation Fellow.

† Supported in part by PHS Research Grant No. GM 14123 from the National Institutes of Health and by the Advanced Research Projects Agency.

[1] P. P. Sorokin, G. J. Lasher, and I. L. Gelles, Phys. Rev. **118**, 939 (1960).

[2] W. P. Unruh and J. W. Culvahouse, Phys. Rev. **129**, 2441 (1963).

[3] P. R. Moran, Phys. Rev. **135**, A247 (1964).

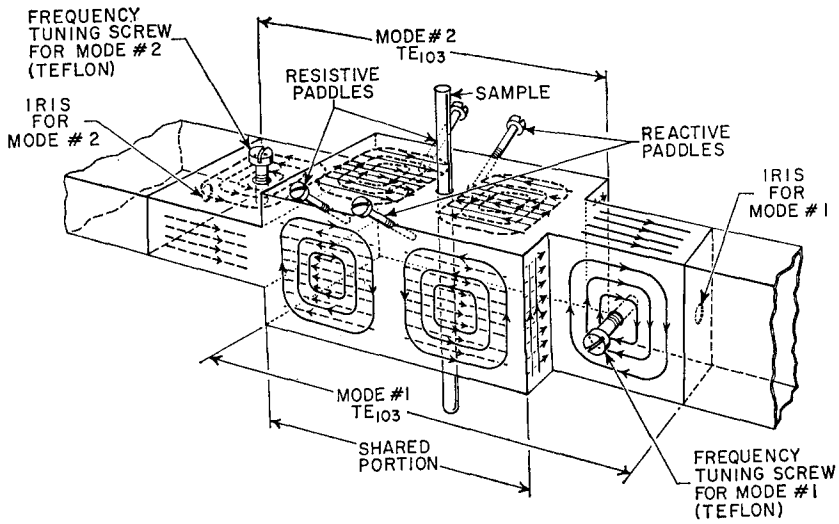


FIG. 1. The prototype bimodal cavity in which two rectangular $TE_{103}$ modes are crossed and have two half-wavelengths common. The lines of rf magnetic flux of mode #1 are indicated by solid lines and of mode #2 by dashed lines.

sented in Sec. III. In Sec. IV a theoretical analysis is developed. A discussion of the experiments and theory is given in Sec. V.

## II. INSTRUMENTATION

### A. The Microwave Cavity

Bimodal cavities have been used not only for electron–electron double resonance experiments, but also for electron paramagnetic resonance (EPR) experiments which are the microwave analogy of the original NMR crossed-coil induction experiments of Bloch, Hansen, and Packard.[4–6]

Design requirements of bimodal cavities for these two uses differ somewhat. In the induction experiment, one requires the crossed cavities to resonate at the same frequency. The problem of spurious coupling between modes is serious. In addition, it is useful to be able to introduce in a controlled manner either a resistive or a reactive coupling between modes in order to detect either absorption or dispersion. Reactive and resistive "paddles" were introduced into the microwave cavities described in Refs. 5 and 6, where the word "paddle" is adopted from the language of nuclear magnetic resonance. These paddles could be used to decouple the two modes and to introduce a slight coupling in a controlled manner.

In electron–electron double resonance, the crossed cavities normally oscillate at different frequencies which tends to reduce undesirable coupling between modes. Moran[3] found that paddles were useful in some of his double electron resonance experiments, but Sorokin *et al.*[1] did not bother to introduce them into their design.

In electron–electron double resonance, provision must be made to tune the resonant frequencies of the two modes with respect to each other. It is desirable to be able to alter the frequency of one mode without affecting the frequency of the other mode. This requirement was satisfied to a fair degree[1–3] by the introduction of dielectric screws which were in an rf electric-field maximum for one mode and an electric-field node for the other (crossed) mode.

Each of the cavities described in the literature is completely degenerate in space, which is to say that the two orthogonal or crossed modes occupy the same volume. Either cylindrical $TM_{011}$ or $TE_{111}$ modes were employed.

In the present work rectangular cavities have been employed which are partially degenerate in space; the crossed resonant modes have a portion of their volume in common and a portion not in common. In order to test some of our cavity design ideas, the cavity of Fig. 1 was made by electroforming over an aluminum mandrel and etching the aluminum away. The two crossed modes of this cavity oscillate in rectangular $TE_{103}$ modes and share two half-wavelengths in common.

In rectangular $TE_{10n}$ modes, the dimension corresponding to the zero subscript does not affect the resonant frequency. For each of the two modes in this cavity there is a step in this dimension with no particular ill effects. One end of each mode is terminated by what is effectively a crossed waveguide. The microwave field does bulge somewhat into this opening, lowering the resonant frequency. Unloaded cavity $Q$'s of 8000 were measured.

The irises are in the "unshared" portions, and thus a fair degree of isolation between the modes is assured automatically. A principal advantage of the partially degenerate cavity is that either resonant mode may be tuned in resonant frequency independent of the other by inserting a dielectric (Teflon) or a conducting rod into that portion not in common.

The two orthogonal modes resonating at the same

[4] F. Bloch, W. W. Hansen, and M. Packard, Phys. Rev. **70**, 474 (1946).
[5] J. J. Faris, Am. J. Phys. **26**, 588 (1958).
[6] D. T. Teaney, M. P. Klein, and A. M. Portis, Rev. Sci. Instr. **32**, 721 (1961).

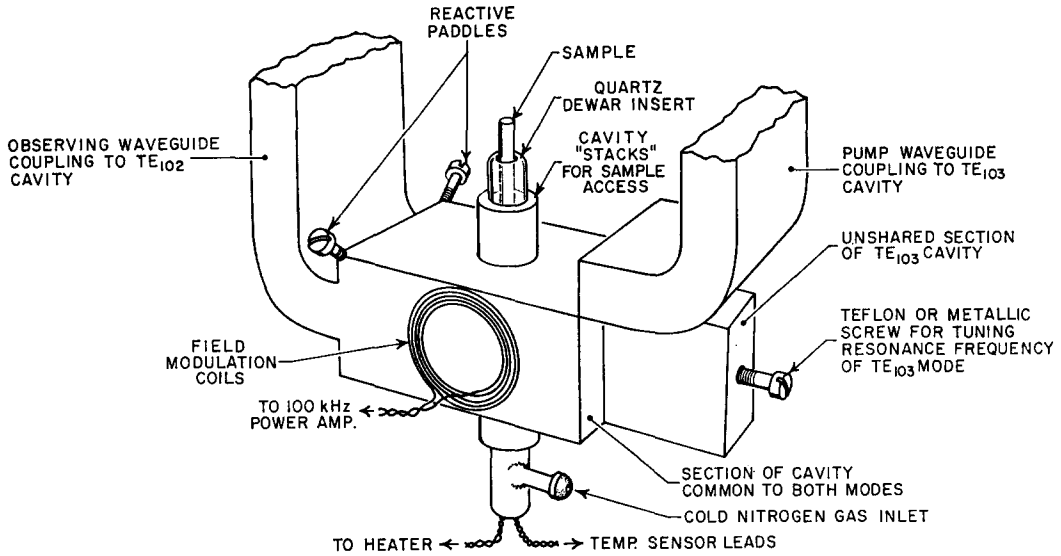


FIG. 2. The bimodal cavity used in this investigation in which a rectangular $TE_{103}$ mode supports the *pumping* microwave field and is crossed with a rectangular $TE_{102}$ mode by which double resonance signals are *observed*.

frequency were isolated by about 30 dB when the cavity of Fig. 1 was first assembled. By the insertion of resistive and reactive paddles as indicated in the figure, the isolation could be increased to 80 dB. The resistive paddles were made of small chips of germanium. A sample tube placed as indicated does not alter the balance of the cavities, but it was noted that the resonant frequencies of the two cavities were shifted by different amounts by the insertion of the sample tube. This is because the electric field along the length of the sample is constant for one mode and varies as a cosine for the other mode.

The cavity actually used by us for electron–electron double resonance was patterned after the structure of Fig. 1 and assembled largely from available commercial (Varian) cavity components. A $TE_{102}$ mode was crossed with a $TE_{103}$ mode, as shown in Fig. 2.

The shared two half-wavelengths were formed by the body of a V-4536 ($B_1$ parallel to $B_0$) cavity. This cavity originally was designed for observing $B_1$ parallel to $B_0$ transitions in photoexcited triplet states in the glass phase. It has a nearly square cross section with two resonant $TE_{102}$ modes. When empty, the $B_1$ parallel to $B_0$ mode resonates at 9.65 GHz while the $B_1$ perpendicular mode resonates at 9.5 GHz. When a quartz Dewar insert is placed in the cavity, the parallel mode shifts to 8.9 GHz and the perpendicular to 9.1 GHz. When used for the triplet-state experiment, an iris is employed which couples equally well to both modes and one may readily go back and forth between modes by changing microwave frequency. In the V-4536 cavity, "stacks" were employed of 11 mm diameter for access of sample tubes and the Dewar insert to the cavity. These stacks are effectively circular waveguides beyond cutoff. A major result of our experience with this cavity was that stacks can be inserted not only in the walls where the microwave electric field is zero amplitude, but also in the sides where the electric field vectors are perpendicular to the wall and terminate there.

The unshared half-wavelength was the top-coupled single section of the V-4534 (optical transmission) cavity. The length of this single section was increased by 5 mm over the usual half-wavelength distance in order to bring the two frequencies nearly into coincidence. Insertion of a $\frac{1}{4}$-in.-diameter Teflon screw into the single section as indicated in Fig. 2 shifted the frequency of the $TE_{103}$ mode lower by several hundred megahertz, and replacement of the Teflon screw by a metallic screw shifted it up in frequency by about 50 MHz.

Since the present experiment is concerned with normal magnetic dipole transitions, it was necessary to place the cavity at an angle with respect to the magnetic field. In this way, there is a component of the rf magnetic field of the $TE_{102}$ mode at right angles to $B_0$. The field-modulation amplitude parallel to $B_0$ was diminished by this rotation, but neither compromise was critical. In the experiments reported here, the $TE_{102}$ mode is referred to as the observing mode and the $TE_{103}$ as the pump mode.

Since the iris of the $TE_{102}$ mode also was exposed to the microwave fields of the $TE_{103}$ mode, more cross coupling was observed than with the test microwave structure of Fig. 1. This coupling could be reduced in a satisfactory manner by use of the reactive "paddles" illustrated in Fig. 2; it was not necessary to use resistive paddles.

### B. The Spectrometer System

The experiment was designed around a V-4502 EPR spectrometer. High-frequency 100-kHz field modulation

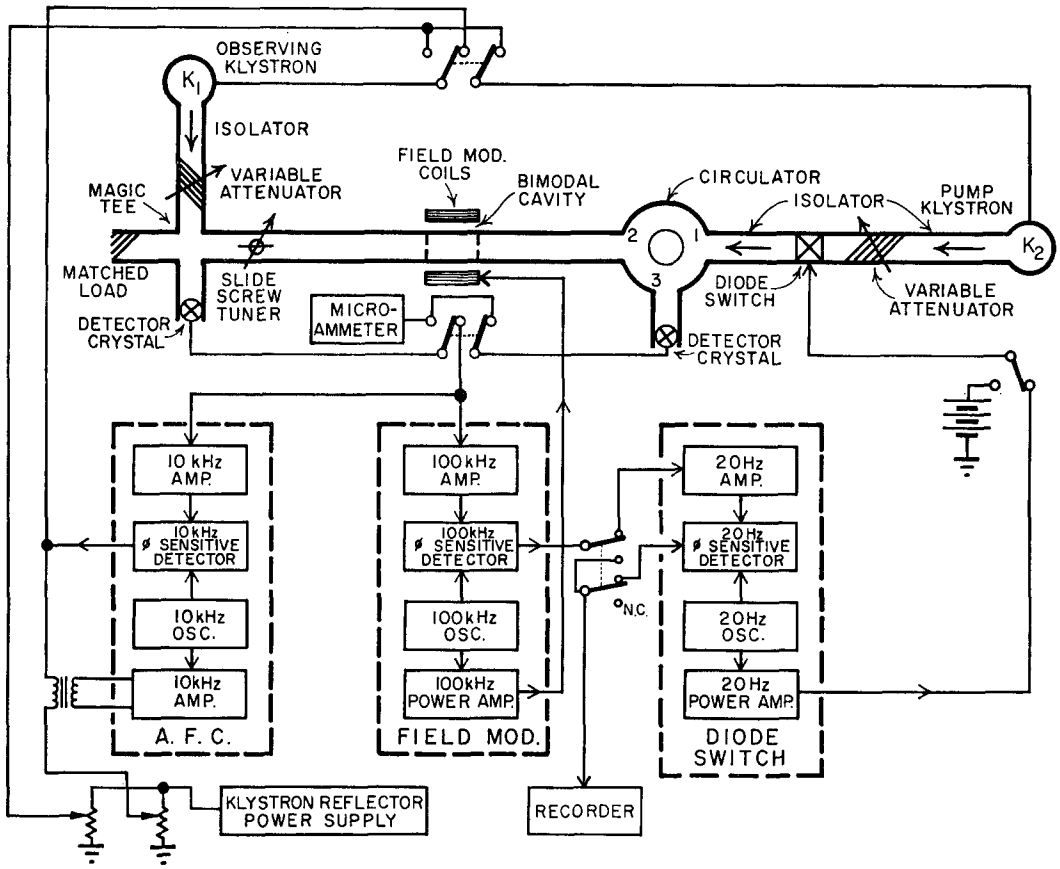


FIG. 3. Block diagram of the equipment.

was employed. A V-4557 variable-temperature Dewar insert passed through the cavity; the cavity being held at room temperature. A V-K3525 (superheterodyne) accessory, somewhat modified, served as a convenient microwave source for the pump mode. A simple bridge was attached to this source so that EPR spectroscopy could be done either by using the pump or the observing microwave source, and in this manner precise alignment of the two microwave frequencies could be achieved. A microwave frequency counter also was helpful in this alignment.

In many of the experiments the pump microwave field was chopped at 20 Hz with a diode switch. Following 100-kHz amplification and phase detection, the observing signal was amplified and phase detected at 20 Hz. This is an electronic means of subtracting the signal obtained in the presence of the pump field from that obtained with only the observing field incident on the sample. The displayed signal in this configuration arises entirely from a double resonance interaction. It was particularly useful under those experimental conditions where the double resonance effect was a very small percentage change of the ordinary EPR signal. Under conditions suitable for optimum double resonance signals, it was more convenient, however, to run separate spectra with and without the pumping field. An experimental convenience of the chopping technique was that it permitted precise balancing of the crossed cavities. The level of the 20-Hz signal reaching the observing crystal in a spurious manner with no magnetic resonance occurring could be monitored and minimized easily.

A block diagram of the equipment is shown in Fig. 3. The resonator, filament, and $B^+$ supplies and the spectrometer oscilloscope are not indicated in the figure. Only the observing klystron was stabilized with an automatic frequency control; the pump klystron had sufficient stability when free running that only occasional adjustments of the reflector voltage were necessary—using the microammeter indicated in the figure to monitor the signal level reflected from the cavity. It is felt, however, that AFC control of the pump klystron would be a desirable improvement in the equipment. Switches permit inverting the pump and observing klystrons. In a first version of the equipment the isolator in front of the diode switch was omitted. A low microwave level from the observing klystron reached the switch in a spurious manner, where it was modulated and reflected. Undesirable effects of this were eliminated by introduction of the isolator.

## III. EXPERIMENTAL

### A. Materials

The compounds which have been used are shown in Fig. 4. Compound I, referred to in the text which

follows simply as the "nitroxide radical,"[7] was investigated in greatest detail. Eastman White-Label ethylbenzene was used as a solvent for most of the nitroxide samples. It was purified by passing through a 15-cm column of freshly activated alumina. Samples were degassed by freezing and pumping several times, except for one experiment where it was desired to check the effect of dissolved molecular oxygen. In order to vary viscosity at constant temperature, some nitroxide samples were prepared in heavy- and light-viscosity mineral oil. These were degassed but not otherwise purified. Compound II, tetracyanoethylene-anion radical (referred to as TCNE), was prepared by reacting TCNE with an excess amount of *N*-ethyl carbazole, using dimethoxyethane (DME) as a solvent. The DME was purified by passing through a column of alumina and, as usual, the samples were degassed by freezing and pumping. The samples of compound III, Coppinger's radical, were prepared several years ago for electron–nuclear double resonance of free radicals in solution.[8] As a solvent, *n*-heptane was used. The samples were degassed and have been stored at $-20$°C. They show no signs of deterioration, but the concentrations are somewhat uncertain.

### B. EPR Characteristics of the Nitroxide Radical

The EPR spectrum of the nitroxide radical in solution consists of three well-resolved equally intense lines 44 MHz apart arising from hyperfine coupling to the $^{14}$N nucleus. Each of these three lines is inhomogeneously broadened[9] by weak interactions with the protons in the molecule. For sufficiently dilute samples ($\approx 10^{-4}$M) and low microwave powers this proton structure can

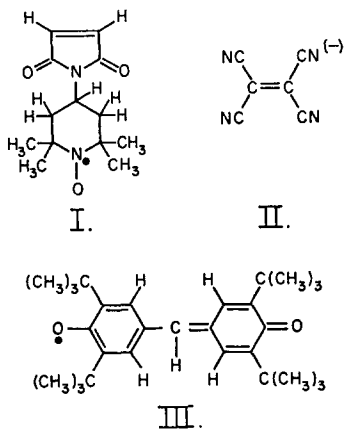


FIG. 4. Compounds used in this investigation: I. 4-*N*-maleimido-2,2,6,6-tetramethyl piperidine nitroxide; II. Tetracyanoethylene-anion radical; III. Coppinger's radical.

[7] This compound 4-N-maleimido-2,2,6,6-tetramethyl piperidine nitroxide was synthesized by H. Stratigos, R. D. Wilcox, and D. E. Green of Varian Associates following a procedure similar to that given by O. H. Griffith and H. M. McConnell, Proc. Natl. Acad. Sci. U.S. **55**, 8 (1966).

[8] J. S. Hyde and A. H. Maki, J. Chem. Phys. **40**, 3117 (1964); J. S. Hyde, *ibid.* **43**, 1806 (1965).

[9] J. H. Freed and G. K. Fraenkel, J. Chem. Phys. **40**, 1815 (1964).


FIG. 5. EPR spectrum of the nitroxide radical, compound I, at $3\times10^{-5}M$ in ethylbenzene at 25°C and an incident microwave power of 5 mW.

be resolved in the temperature range of $-70$° to $+45$°C in ethylbenzene. At least nine lines can be seen with a coupling constant of 1.17 MHz. Presumably this is the coupling to the 12 equivalent methyl protons. An EPR spectrum is shown in Fig. 5. All of the electron–electron double resonance spectra reported here were obtained at high microwave powers and were overmodulated such that no proton hyperfine structure was observed.

Preliminary experiments indicated that the magnitude of the electron–electron double resonance signals from the nitroxide radical was critically dependent on the level of the pump power and that this level should be 50 to 100 mW for optimum signals. On the other hand, it was found that the observing microwave level was not as critical. It was for this reason that the $TE_{103}$ mode was used as the pump mode. The rf magnetic field $B_1$ of this mode is perpendicular to $B_0$, and the circulator in the bridge (Fig. 3) gives a factor of 2 more power at the sample. The maximum available component of the rf field at the sample in the observing mode and perpendicular to $B_0$ is substantially less. The angle of $B_1$ with respect to $B_0$ of the observing $TE_{102}$ cavity mode is approximately 25°. Thus for comparable levels of saturation in the pump and observing modes, the incident powers must differ by about a factor of $\sin^2 25°$, which is 0.17.

Microwave power saturation characteristics were determined for $10^{-4}M$ nitroxide. Because of linewidth effects which arise from imperfect averaging of anisotropic interactions, the three nitrogen hyperfine lines saturate differently at lowest temperature. Saturation curves at $-90$°C were obtained for the $+1$ and $-1$ lines. See Fig. 6. The low-field ($+1$) line is more intense (and narrower) and saturates more readily than the high-field ($-1$) line, as expected.[9] Saturation curves for higher temperatures, observing the $+1$ hyperfine line, are shown in Fig. 7. These data were obtained from the pump microwave bridge coupled to the $TE_{103}$ cavity mode.

These saturation curves have the typical form for

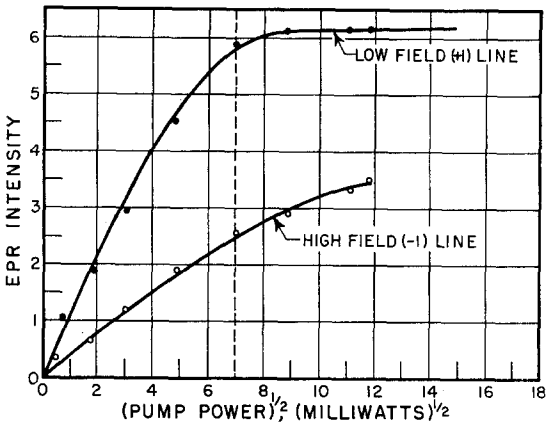


FIG. 6. Microwave power saturation curves for the $TE_{103}$ *pump* mode for $10^{-4}M$ nitroxide in ethylbenzene at $-90°C$. The dashed line on the figure indicates the maximum degree of saturation which can be obtained for the $TE_{102}$ *observing* mode.

inhomogeneous lines.[10] It is not possible in a straightforward manner to separate the transverse and longitudinal relaxation times. However, the observation that proton hyperfine structure can be resolved in the temperature range of $-70$ to $+45°C$ indicates that the transverse relaxation time has a broad maximum and changes relatively little in the temperature interval employed in these experiments. Thus from Fig. 7 it is concluded that the longitudinal relaxation time decreases as the temperature is increased. The ease with which saturation occurs decreases at higher concentrations, and no saturation was observed in samples which had not been degassed. The maximum level of saturation which can be reached in the observing mode is indicated on Figs. 6 and 7 by a dashed line.

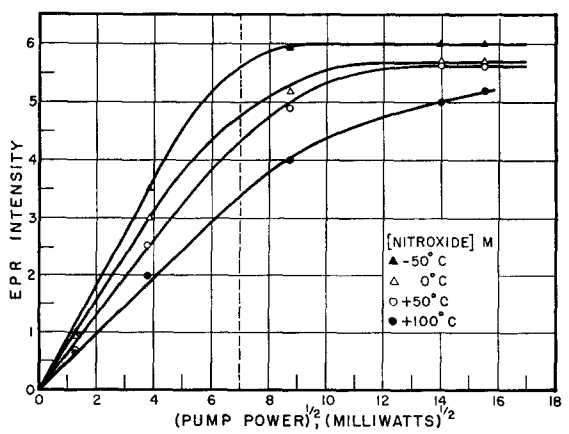


FIG. 7. Microwave power saturation curves obtained on the low-field $(+1)$ line of $10^{-4}M$ nitroxide in ethylbenzene at several temperatures. The $TE_{103}$ *pump* mode was used; the dashed line on the figure indicates the maximum degree of saturation which can be obtained for the $TE_{102}$ *observing* mode.

[10] A. M. Portis, Phys. Rev. 91, 1071 (1953).

### C. Optimum Double Resonance Effects in the Nitroxide Radical

The signal-to-noise ratio of the electron–electron double resonance signals of the nitroxide radical in ethylbenzene was highest just above the freezing point with both the pump and observing microwave levels near the maxima available. The ordinary EPR spectra of the nitroxide radical are shown in Fig. 8(a). EPR spectra are shown in Fig. 8(b) with the pump klystron turned on and adjusted first to 44 MHz below the observing frequency klystron and then 44 MHz above; the spectra of Fig. 8(c) were obtained by chopping the pump amplitude as described in the instrumental section and are effectively spectra 8(b) subtracted from spectra 8(a). In this magnetic field sweep, two hyperfine lines are affected. The third, of course, is

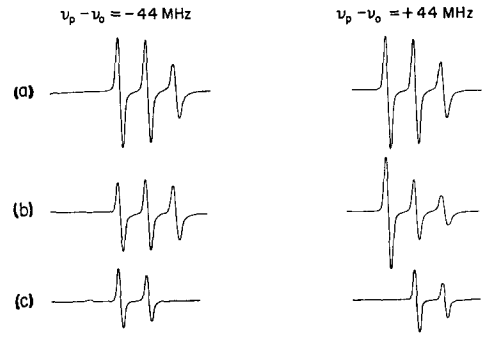


FIG. 8. (a) Ordinary EPR spectra of $10^{-4}M$ nitroxide radical in ethylbenzene at $-80°C$ and maximum available observing microwave power. (b) The EPR spectra at the same conditions as (a) but with the pump turned on at maximum available microwave power and the pump frequency set first to *one* hyperfine separation below and then to *one* hyperfine separation above the observing microwave frequency. (c) The electron–electron double resonance spectra: effectively (b) subtracted from (a).

unaffected since when it is observed, the pump no longer is on a hyperfine inverval. When $(\nu_p - \nu_o)$ did not correspond to an integral multiple of the hyperfine separation, little or no effect was obtained.

In Fig. 9(a), 9(b), 9(c), electron–electron double resonance spectra of the nitroxide radical are shown for $\nu_p - \nu_o = \pm 88$ MHz. As expected, the difference spectrum, Fig. 9(c), shows a single line arising when the pump is at one end of the spectrum and the observing mode on the other. Figures 8 and 9 were obtained at $-80°C$ and $10^{-4}M$ nitroxide radical.

We note by comparing traces (a) with traces (b) that there is a reduction of the observed signal amplitude when the pump is turned on. In the discussion which follows, it is convenient to speak of a reduction factor $R$, which is defined as [(signal with pump off) − (signal with pump on)]/(signal with pump off). The values of $R$ obtained from the data of Figs. 8 and 9 are given in Table I.A.

### D. Variation of Temperature and Concentration

In Fig. 10 we plot the reduction, $R$, as a function of temperature at several concentrations of the nitroxide radical. Both the pump and observing power levels were near the maxima available. All points in this figure were obtained by observing the low-field ($M_I=+1$) line and pumping the center ($M_I=0$) interval. This plot indicates clearly that at least two mechanisms are operative which give electron–electron double resonance signals from free radicals in solution. At lowest temperatures all samples from $10^{-2}$ to $3\times10^{-5}M$ yield substantially the same reductions. The reduction factor $R$ decreases as the temperature is increased, and for the most dilute sample, $3\times10^{-5}M$, no double resonance effects could be detected above 0°C. However, for more concentrated samples, easily observable reductions could be seen at higher temperatures, and the magnitude of the effect was very dependent on concentration, but independent of temperature. The higher the concentration the greater is the value of $R$ in the high temperature range. The reduction becomes temperature independent at lower temperatures for more concentrated samples. The temperature-independent values of $R$ obtained were $10^{-2}M$, 0.20; $10^{-3}M$, 0.08; $3\times10^{-4}M$, 0.03.

These results are consistent with an intramolecular and hence concentration-independent mechanism at lowest concentrations and temperatures, and an intermolecular or concentration-dependent mechanism at high concentrations and temperatures where encounters between molecules are more frequent.

Since some differences were found in the reductions obtained at −80°C depending on which hyperfine line was observed and which interval was pumped, similar data were obtained at higher temperatures. The results are given in Table I. We will return to these data when we compare theory and experiment in Sec. V.

TABLE I. Reduction factors, $R$, for $10^{-4}M$ nitroxide.

| Line pumped | Line observed +1 | 0 | −1 |
|---|---|---|---|
| A. −80°C | | | |
| +1 | ··· | 0.42 | 0.285 |
| 0 | 0.382 | ··· | 0.465 |
| −1 | 0.225 | 0.322 | ··· |
| B. −50°C | | | |
| +1 | ··· | 0.216 | 0.061 |
| 0 | 0.226 | ··· | 0.222 |
| −1 | 0.072 | 0.203 | ··· |
| C. −20°C | | | |
| +1 | ··· | 0.095 | 0.033 |
| 0 | 0.109 | ··· | 0.10 |
| −1 | 0.03 | 0.10 | ··· |
| D. +10°C | | | |
| +1 | ··· | 0.030 | 0.019 |
| 0 | 0.034 | ··· | 0.031 |
| −1 | 0.017 | 0.024 | ··· |

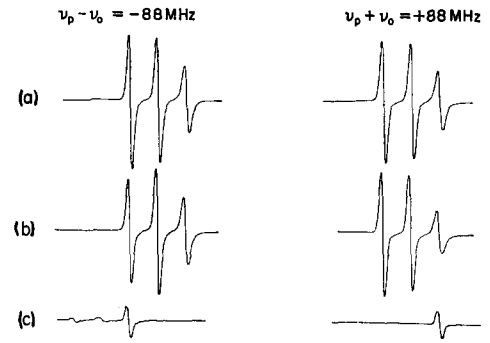


FIG. 9. (a) Ordinary EPR spectra of $10^{-4}M$ nitroxide radical in ethylbenzene at −80°C and maximum available observing microwave power. (b) The EPR spectra at the same conditions as (a) but with the pump turned on at maximum available microwave power and the pump frequency set first to *two* hyperfine separations below and then to *two* hyperfine separations above the observing microwave frequency. (c) The electron–electron double resonance spectra: effectively (b) subtracted from (a).

### E. Electron-Electron Double Resonance Involving Proton Hyperfine Couplings

Thus far all results reported here have been for nitrogen hyperfine couplings. To study electron–electron

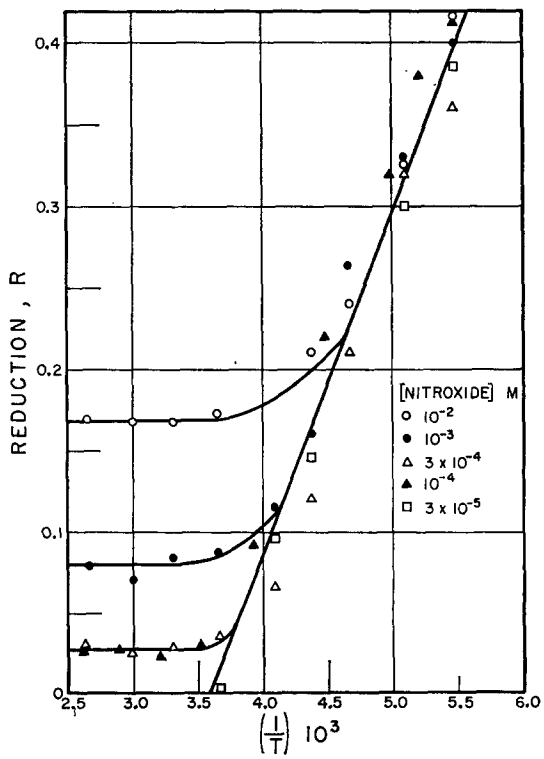


FIG. 10. Reduction, $R$, as a function of temperature at several concentrations of the nitroxide radical in ethylbenzene. The low-field ($M_I=+1$) line was observed and the central ($M_I=0$) interval was pumped.

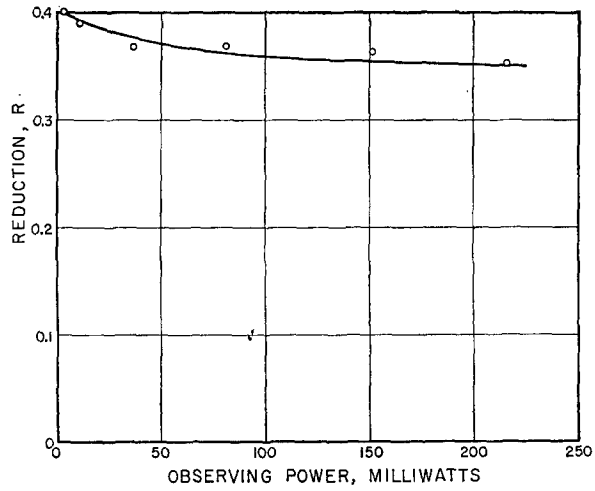


FIG. 11. Dependence of the electron-electron double resonance reduction, $R$, on the observing microwave power level for $10^{-4}M$ nitroxide in ethylbenzene at $-80°C$ with a strongly saturating pump level. The low-field ($M_I=+1$) line was observed and the central ($M_I=0$) interval was pumped.

double resonance of protons, Coppinger's radical was examined. This radical has a coupling of 15.6 MHz to the central proton and 3.8 MHz to the four equivalent ring protons. In our experiments the two microwave frequencies were separated by 15.6 MHz. The results may be summarized by the observation that the intramolecular mechanism, found to be important for nitrogen couplings, is of much reduced importance. On the other hand, the intermolecular mechanism gives larger values of $R$ than found for the nitroxide radical at comparable concentrations and temperatures. The reductions we found for $3\times10^{-4}$, $10^{-4}$, and $3\times10^{-5}M$ Coppinger's radical in $n$-heptane at $-85°C$ were 0.345, 0.195, and 0.10. These values were obtained with pump and observing microwave power levels at the maxima available. The values of $R$ decreased somewhat as the temperature was raised, suggesting a weak intramolecular mechanism, but quickly approached a temperature-independent value. For example, the $10^{-4}M$ sample gives a temperature-independent reduction, $R$, of 0.11 between 40° and $-50°C$ which increases to 0.195 at $-85°C$.

### F. Variation of Microwave Power Levels

The dependence of the double resonance reduction on the observing microwave power is shown in Fig. 11. This curve was obtained on a $10^{-4}M$ solution of the nitroxide radical at $-80°C$ with the pump power near a maximum and strongly saturating. The low-field ($+1$) line was observed and the central ($M_I=0$) line was pumped. The value of $R$ decreases somewhat as the observing microwave power approaches saturation. Unfortunately it was not possible with the equipment assembled here to carry this plot into the region of strongly saturating observing power.

The dependence of the double resonance reduction on the pumping microwave power is shown in Fig. 12. This curve was obtained on the nitroxide radical at $10^{-4}M$ and $-80°C$, with the observing power near the maximum available. Again the low-field ($+1$) line was observed and the central ($M_I=0$) line was pumped. The form of the display of these data anticipates the theoretical development of Sec. IV. From this curve it is apparent that for maximum effect the maximum available pump power should be used. The maximum effect which can be obtained (i.e., the inverse of the intercept of Fig. 12) is $R_{max}=0.45$, and this level is approached in the limit of strong saturation by the pump microwave field.

Coppinger's radical saturates very much more easily than does the nitroxide radical. Microwave levels for a comparable degree of saturation differ by about 15 dB for the two radicals. Anticipating the results of Secs. IV and V, this difference appears to be the dominant factor in explaining the observation that the reduction, $R$, obtained on concentrated samples in the temperature-independent region is much greater for Coppinger's radical than for the nitroxide radical.

Coppinger's radical was used to investigate the effect of pump microwave power on the electron–electron double resonance signal obtained in the temperature-independent region where the intermolecular mechanism dominates. The results are shown in Fig. 13. The

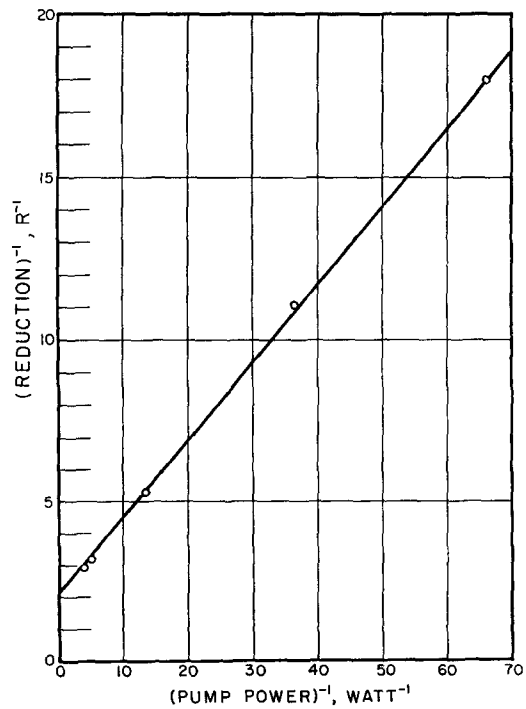


FIG. 12. Dependence of the electron-electron double resonance reduction, $R$, on the pumping microwave power level for $10^{-4}M$ nitroxide in ethylbenzene at $-80°C$ with the observing power near the maximum available. The low-field ($M_I=+1$) line was observed and the central ($M_I=0$) interval was pumped.

reduction factor $R$ is seen to approach a constant level as the microwave pump power is increased.

### G. Microwave Frequencies Two and More Hyperfine Intervals Apart

The results shown in Figs. 8, 9, and Table I suggested that it would be useful to determine $R$ when $(\nu_p-\nu_o)$ corresponds to higher integral multiples of the hyperfine splitting, and for this purpose two systems were investigated, TCNE-anion radical and DPPH.

The EPR spectrum of TCNE-anion radical has nine principal hyperfine lines 4.3 MHz apart arising from 4 equivalent nitrogen nuclei. On the average, $R$ decreases by a factor of 1.5 for each increase in the separation of the two klystron frequencies by one hyperfine interval. This result was obtained at $10^{-4}M$, $-80$°C in DME.

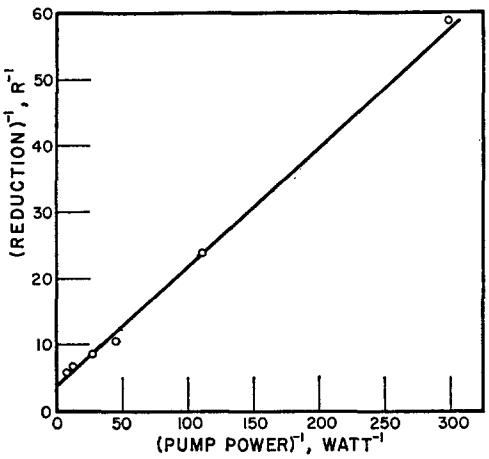


FIG. 13. Dependence of the electron–electron double resonance reduction, $R$, on the pumping level for $10^{-4}M$ Coppinger's radical at +25°C with the observing microwave power strongly saturating. The two microwave frequencies were separated by 15.6 MHz.

The EPR spectrum of DPPH has 5 principal hyperfine lines arising from contact with two nearly equivalent nitrogen nuclei. Each line is considerably broadened by weaker proton interactions. The value of $R$ decreased by a factor of 1.8 for each increase in the separation by one hyperfine interval, with the possible exception of the case where the two frequencies were separated by four intervals. The data for TCNE and DPPH are shown in Tables II and III.

Since it had been established that there are apparently two operative mechanisms for the observation of electron–electron double resonance of free radicals in liquids, it was of interest to see whether or not the observed decrease in $R$ with increasing number of hyperfine intervals applied to both. In all cases at high concentration and high temperature where the intermolecular mechanism is dominant, the observed reductions were independent of the number of hyperfine intervals separating the two frequencies.

TABLE II. Reduction, $R$, as a function of pumping frequency for $10^{-4}M$ DPPH in ethylbenzene at $-80$°C.

| $\nu_o-\nu_p$(MHz) | $R$ |
|---|---|
| 25.1 | 0.33 |
| 50.0 | 0.18 |
| 75.0 | 0.10 |
| 100.0 | 0.03 |

### H. Miscellaneous Experiments

Several miscellaneous experiments were performed which should be reported. The first of these involved a systematic variation of the separation of the two frequencies through the hyperfine coupling. The electron–electron double resonance effect was a maximum when the frequencies coincided, and the effect was diminished by half when the frequencies differed by $(44\pm\Delta)$ MHz, where $\Delta$ is the full width at half-height of the EPR line and equals 7 MHz for the nitroxide line.

In the difference mode of display the line shapes are distorted, resembling dispersive curves, when the separation of the frequencies is slightly off. A good line shape in the difference mode indicates that the separation of the two frequencies has been set correctly. This observation may be useful in analysis of complex spectra by electron–electron double resonance.

Several experiments were performed using solvents of different viscosities and the results are summarized in Table IV. These experiments indicate that the intramolecular mechanism observable in ethylbenzene at low temperatures and concentrations is dominant at higher temperatures and concentrations if the viscosity is higher.

Several different experiments were attempted under various conditions on samples which had not been degassed. In all cases the presence of oxygen effectively eliminates double resonance signals.

## IV. THEORY OF ELECTRON–ELECTRON DOUBLE RESONANCE

The theoretical analysis of electron–electron double resonance is based on the general theory of steady-state multiple resonance EPR experiments that has been

TABLE III. Relative reductions as a function of pumping frequency for $10^{-4}M$ TCNE anion radical in dimethoxyethane at $-80$°C.

| $\nu_o-\nu_p$(MHz) | Relative intensity of double resonance difference spectra |
|---|---|
| 4.46 | 0.74 |
| 8.72 | 0.31 |
| 13.02 | 0.14 |
| 17.34 | 0.08 |
| 21.73 | 0.04 |

TABLE IV. Dependence of reduction[a] on viscosity of medium.

| Concentration ($M$) | $R$ | | |
|---|---|---|---|
| | Ethylbenzene | Light-viscosity mineral oil | High-viscosity mineral oil |
| $3\times10^{-5}$ | 0 | 0.15 | 0.38 |
| $10^{-4}$ | 0.034 | 0.18 | 0.39 |
| $3\times10^{-4}$ | 0.023 | 0.15 | 0.38 |

[a] Nitroxide radical at 25°C, $\nu_o-\nu_p=44$ MHz.

developed elsewhere.[11-13] The basic result is that instead of describing the spectrum in terms of an individual saturated Lorentzian for each hyperfine line or component thereof, one obtains coupled saturated Lorentzians which are best formulated in matrix notation. Thus we define a vector $\mathbf{Z}''$ in "transition space" such that each component corresponds to an induced absorption mode of a particular spin transition. These modes are proportional to the components of the magnetization which are observed in ordinary resonance experiments. The matrix solution for $\mathbf{Z}''$ is[11-13]

$$\mathbf{Z}''=\mathbf{M}^{-1}(-\mathbf{R}^{-1})\mathbf{Q}, \tag{1}$$

where

$$\mathbf{M}=\mathbf{1}+(\mathbf{R}^{-1}\mathbf{K})^2+(-\mathbf{R}^{-1})\mathbf{S}. \tag{2}$$

We assume, for simplicity, at the outset that in the double EPR experiment one pumps on a simple Lorentzian line and observes another simple line. This is the case for a radical with a single nucleus of spin $I$. (When there are several equivalent nuclei, there will be composite hyperfine lines, and the present treatment can be extended to such cases using the methods in Refs. 11 and 12.) Thus we have a two-dimensional transition space with a $Z_o''$, the observing EPR absorption mode, and a $Z_p''$, the pumping EPR mode. We note that these two modes represent *different* hyperfine transitions. The $\mathbf{R}$ matrix is taken to be diagonal for present purposes and consists of $-R_o^{-1}=T_o$ and $-R_p^{-1}=T_p$, the transverse relaxation times for the two induced absorption modes. The $\mathbf{K}$ matrix is also diagonal and consists of the frequency deviations from resonance: $\Delta\omega_o$ and $\Delta\omega_p$, respectively. The $\mathbf{Q}$ vector contains the population differences associated with the transitions. The only coupling between the two modes arises from the off-diagonal elements in the $\mathbf{S}$ matrix. (The diagonal elements of the $\mathbf{S}$ matrix are given by $d_o^2\Omega_o$ and $d_p^2\Omega_p$, respectively, where $d_o$ and $d_p$ are the transition moments given for spins of $\frac{1}{2}$ by $d_i=\frac{1}{2}\gamma_e B_i$ with $B_i$ the circularly rotating component of microwave magnetic field and $\gamma_e$ the magnetogyric ratio of the electron, and $\Omega_o$ and $\Omega_p$ are the saturation parameters.) This coupling yields two effects:

Effect (1) is a polarization effect which results from the fact that an intense pumping field readjusts the populations of the levels between which the observing transition occurs. This is not unlike an Overhauser effect. However, in the present case the two transitions of interest have no level in common, and this leads to special requirements on the relaxation processes in order to obtain significant effects. Also nuclear polarization plays no role in the EPR experiment.

Effect (2) is important *only* when $Z_o''$ is being saturated. It reflects the fact that the induced absorption mode $Z_p''$ acts as an induced transition which, in conjunction with lattice-induced transitions, can facilitate the rate of energy transferred from the observing radiation field to the lattice via the spin systems. It is closely analogous to the ENDOR mechanism discussed elsewhere.[11-13]

The two coupled equations we obtain from Eqs. (1) and (2) are

$$Z_o''=d_oT_oq\omega_o(M^{-1})_{o,o}+d_pT_pq\omega_p(M^{-1})_{o,p}, \tag{3a}$$

$$Z_p''=d_pT_pq\omega_p(M^{-1})_{p,p}+d_oT_oq\omega_o(M^{-1})_{p,o} \tag{3b}$$

with

$$M=\begin{pmatrix}1+\Delta\omega_o^2T_o^2+d_o^2T_o\Omega_o & d_od_p\Omega_{o,p}T_o\\ d_pd_o\Omega_{p,o}T_p & 1+\Delta\omega_p^2T_p^2+d_p^2T_p\Omega_p\end{pmatrix}, \tag{4}$$

where $q=\hbar/kT$, and $\Omega_{o,p}$, etc., are cross-saturation parameters.

The solution for $Z_o''$ is:

$$Z_o''=q\omega_eT_od_o\left[\frac{1-\xi_o/\Omega_{p,o}}{1+\Delta\omega_o^2T_o^2+d_o^2T_o(\Omega_o-\xi_o)}\right] \tag{5}$$

with

$$\xi_o=d_p^2T_p\Omega_{o,p}\Omega_{p,o}/(1+\Delta\omega_p^2T_p^2+d_p^2T_p\Omega_p), \tag{6}$$

where we have set $\omega_o=\omega_p=\omega_e=|\gamma_e|B$ consistent with the general approximation of neglecting nuclear Zeeman and hyperfine energies compared to the electron-spin Zeeman energy in a dc field of strength $B$. The polarization effect is given by the second term in the numerator of Eq. (5), while the induced transition effect is given by $\xi_o$ in the denominator.

It is interesting to obtain some special cases of Eqs. (5), (6). Thus for exact resonance, $\Delta\omega_p=0$, and very strong saturation of the pumping transition:

$$d_p^2T_p\Omega_p\gg1,$$

one obtains:

$$\xi_o^r(d_p^2\to\infty)=\Omega_{o,p}\Omega_{p,o}/\Omega_p \tag{7}$$

[11] J. H. Freed, J. Chem. Phys. **43**, 2312 (1965).
[12] J. H. Freed, J. Phys. Chem. **71**, 38 (1967).
[13] J. H. Freed, D. S. Leniart, and J. S. Hyde, J. Chem. Phys. **47**, 2762 (1967).

so that

$$\bar{Z}_o''=q\omega_e T_o d_o\left[\frac{(\Omega_p-\Omega_{o,p})/\Omega_p}{1+T_o^2\Delta\omega_o^2+d_o^2T_o(\Omega_o\Omega_p-\Omega_{o,p}\Omega_{p,o})/\Omega_p}\right], \tag{8}$$

where the bar over $Z$ implies the limit of Eq. (7). The positive and negative terms in the numerator of Eq. (8) are from the first and second terms, respectively, in Eq. (5). If a "generalized no-saturation" condition exists:

$$d_o^2T_o[(\Omega_o\Omega_p-\Omega_{o,p}\Omega_{p,o})/\Omega_p]\ll 1,$$

then Eq. (8) reduces to

$$\bar{Z}_o''=[T_o\omega_e q d_o/(1+T_o^2\Delta\omega_o^2)][1-(\Omega_{o,p}/\Omega_p)]. \tag{9}$$

If a "generalized strong-saturation" condition holds:

$$d_o^2T_o[(\Omega_o\Omega_p-\Omega_{o,p}\Omega_{p,o})/\Omega_p]\gg 1,$$

then Eq. (8) reduces, for $\Delta\omega_o=0$, to

$$\bar{Z}''^r=\frac{q\omega_e}{d_o}\left(\frac{\Omega_p-\Omega_{o,p}}{\Omega_o\Omega_p-\Omega_{o,p}\Omega_{p,o}}\right)\rightarrow\frac{q\omega_e}{d_o}(\Omega_o+\Omega_{o,p})^{-1}$$
$$\text{as } \Omega_{o,p}\rightarrow\Omega_{p,o} \text{ and } \Omega_p\rightarrow\Omega_o. \tag{10}$$

Both Eqs. (9) and (10) represent a reduction of the EPR signal when $\Omega_{o,p}$ is positive. The cross-saturation parameter $\Omega_{o,p}$ is determined solely by the spin–relaxation processes and represents an "impedance" giving the effect on the observing transition from an external disturbance (e.g., a resonant rf field) on the pumping transition.[14a] In effect, a positive $\Omega_{o,p}$ means that the spin–relaxation processes transmit the saturation of the pumped hyperfine line to the observed line. This effect is most evident in the limiting, but not too realistic case that the lattice-induced nuclear spin-flip transition probabilities, $W_n$, are very much greater than the lattice-induced electron spin-flip probabilities, $W_e$. This case is illustrated in Fig. 14. The saturating pumping field sets $P_a=P_b$, where $P_i$ is the probability of being in the $i$th spin state. The strong $W_n$ sets $P_a=P_c$ and $P_b=P_d$ (again neglecting nuclear Zeeman and hyperfine energies). Thus $P_c=P_d$ and the observed transition is fully saturated.[14b] This case will be seen to be equivalent to $\Omega_{o,p}=\Omega_o=\Omega_p$ so that Eq. (9) becomes appropriate

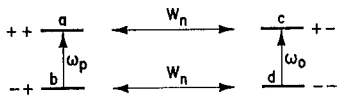


FIG. 14. The limiting electron–electron double resonance case.

for all values of $d_o$. The effect of a finite $W_e$ is to reduce this indirect saturation mechanism so that it is still possible to perform a direct saturation governed by Eq. (10). As already noted, the pumping field will also have an induced transition effect which tends to enhance the saturated signal, and this is also included in Eq. (10).

Previous theoretical[11–13,15,16a] and experimental[9,16b,17,18] analysis has shown that the important spin–relaxation mechanisms in the EPR of dilute, low-temperature solutions of free radicals at X band include $g$-tensor and spin–rotational effects which contribute to the $W_e$ independent of the particular hyperfine transition and electron–nuclear dipolar (END) effects which contribute mainly to $W_n$. However, in less dilute and warmer solutions, chemical-exchange and Heisenberg-exchange processes will also be important.[12] Both exchange processes lead to identical observables in an EPR experiment[12] so that we may introduce an exchange frequency $\omega_{EX}\equiv\omega_{HE}+\omega_{CE}$, where $\omega_{HE}$ and $\omega_{CE}$ are the Heisenberg- and chemical-exchange frequencies, respectively. The effect of $\omega_{EX}$ is to try to equalize the population differences between all pairs of hyperfine levels, and this may be regarded as a source of pseudo-nuclear spin flips. The methods of calculating the $\Omega$'s in terms of all these relaxation processes are discussed in Refs. 11 and 12. It is easy to show, in general, that in the absence of exchange effects $\Omega_{i,j}=\Omega_{j,i}$.[11] This symmetric relation has also been found to be true in all cases involving exchange that have been worked out in detail,[12] including those discussed below.

### A. Single Nucleus of $I=\frac{1}{2}$

Here there are only two EPR transitions which may be induced. One obtains:

$$\Omega_o=\Omega_p=W_e^{-1}[(2+c)/(1+c)], \tag{11a}$$

$$\Omega_{o,p}=W_e^{-1}[c/(1+c)], \tag{11b}$$

where $c=b+b'$ and $b=W_n/W_e$, $b'=\omega_{EX}/2W_e$. Thus $W_n$ and $\omega_{EX}$ have identical effects on the $\Omega$'s in this case. Now from the unsaturated case, Eq. (9), we obtain for $\Delta\omega_o=0$,

$$\bar{Z}_{DEPR}''^r/\bar{Z}_{EPR}''^r=1-(\Omega_{o,p}/\Omega_p)=2/(2+c) \tag{12}$$

which is a reduction, and as $c\rightarrow\infty$ the double resonance

[14] (a) In this point of view, the $\Omega_o$ and $\Omega_p$ terms, which are closely related to the familiar $T_1$'s or longitudinal-relaxation times, represent self impedances expressing the resistance of the particular hyperfine line to adjust to an external disturbance applied directly to it. In the limit, when relaxation coupling between different hyperfine lines is negligible, $\Omega_i=4T_{1,i}$. (b) One may visualize the reverse situation where instead of a strong $W_n$, there are strong $W_x$ or cross relaxations between levels $a$ and $d$ and between $b$ and $c$. In the limit where $W_e\ll W_x$, there is a 100% *enhancement* of the observed transition. The general requirement of an enhancement is that $W_x>W_n$, and this is not realistic for free radicals in solution which can give rise to double resonance effects, see text. It should be noted that if a $W_x$ existed only between one pair of levels (e.g., $b$ and $c$, which would result from modulation of the isotropic hyperfine interaction), then it is found that $\Omega_{o,p}=0$, and there are no observable electron–electron double resonance effects.

[15] J. H. Freed and G. K. Fraenkel, J. Chem. Phys. **39**, 326 (1963).

[16] (a) P. W. Atkins and D. Kivelson, J. Chem. Phys. **44**, 169 (1966); (b) R. Wilson and D. Kivelson, *ibid.* **44**, 154 (1966).

[17] J. W. H. Schreurs and G. K. Fraenkel, J. Chem. Phys. **34**, 756 (1961).

[18] J. S. Hyde and H. W. Brown, J. Chem. Phys. **37**, 2053 (1962).

TABLE V. Saturation factors[a] for a single nucleus of $I=1$.

| | END+exchange | END only[b] | Exchange only[c] |
|---|---|---|---|
| $n\phi_{\pm}$ | $(1+3b'')(1+b'')+b(b+4b''+3)$ | $(1+3b+b^2)$ | $(1+b'')$ |
| $n\phi_c$ | $(1+3b'')(1+b'')+b(b+4b''+2)$ | $(1+2b+b^2)$ | $(1+b'')$ |
| $n\phi_{\pm,c}$ | $(b+b'')(b+3b''+1)$ | $b(1+b)$ | $b''$ |
| $n\phi_{\pm,\mp}$ | $(b^2+b'')(4b+3b''+1)$ | $b^2$ | $b''$ |
| $n$ | $(b+3b''+1)(3b+3b''+1)$ | $(1+b)(1+3b)$ | $(1+3b'')$ |

[a] See Eq. (14).
[b] $b=W_n/W_e$.
[c] $b''=\omega_{EX}/6W_e$.

signal goes to zero as expected. When the observing transition is highly saturated, we obtain from Eq. (10):

$$\bar{Z}_{DEPR}''^{r}/\bar{Z}_{EPR}''^{r}=[1+(\Omega_{o,p}/\Omega_o)]^{-1}$$
$$=\tfrac{1}{2}[(2+c)/(1+c)]. \quad (13)$$

For $c=1$, Eq. (12) yields a $33\frac{1}{3}\%$ reduction, while for Eq. (13) it is reduced to 25%. For cases of intermediate saturation of observing and/or pumping transitions, the more general Eqs. (5) and (6) must be used.

### B. Single Nucleus of $I=1$

Here we have a choice of pumping and observing transitions. Let us label the transitions: $+$, $-$, and $c$ corresponding to the $M_I=+1$, $-1$, and 0 hyperfine components, respectively. The saturation parameters for this case are given in Table V. Note that

$$\Omega_{i,j}=2W_e^{-1}\varphi_{i,j}. \quad (14)$$

Also, in this case the actual nuclear spin–transition probability induced by an END mechanism is $2W_n$, where $W_n$ is the appropriate value if the spin were $I=\frac{1}{2}$. One notes that the saturation factors for exchange-only are independent of the particular hyperfine line(s), but this is not the case for END-only. The reduction factors $R$ are given in Tables VI and VII for unsaturated [Eq. (9)] and strongly saturated [Eq. (10)] observing signals, respectively. Again, the effect for exchange only is independent of the particular hyperfine lines involved, but this is not true of END only, so this is a distinguishing feature between the two mechanisms. This feature arises because the END mechanism only gives rise to $\Delta M_I=\pm 1$ transitions,[11] while exchange may be thought of as giving equal transition probabilities for $\Delta M_I=\pm 1$ and $\pm 2$.[12] Analysis of Tables VI and VII indicates that $R$ is diminished for strong saturation as compared to no saturation.

### C. Temperature Dependence of Reductions

The temperature dependences of the important spin–relaxation mechanisms follow from the equations for their associated transition probabilities. Thus for $g$-tensor and spin–rotational mechanisms, we may write[11,15,19]

$$W_e^{G}=[\sum_i (g_i-g_e)^2/40][(\omega_e^2\tau_R/(1+\omega_e^2\tau_R^2)] \quad (15)$$

and[12,16a]

$$W_e^{SR}=\sum_i (g_i-g_e)^2/18\tau_R, \quad (16)$$

where $g_i$ is the $i$th$=x$, $y$, $z$ component of the $g$ tensor, $g_e=\frac{1}{3}\sum_i g_i$, $g_e$ is the free-electron $g$ value, and $\tau_R$ is an isotropic rotational correlation time given in the Stokes–Einstein model by

$$\tau_R=4\pi\eta a^3/3kT, \quad (17)$$

where $\eta$ is the viscosity and $a$ is the molecular radius. We note from Eqs. (15) and (16) that the ratio of these two mechanisms is:

$$W_e^{G}/W_e^{SR}=0.45[\omega_e^2\tau_R^2/(1+\omega_e^2\tau_R^2)]$$
$$\times[\sum_i (g_i-g_e)^2/\sum_i (g_i-g_e)^2]. \quad (18)$$

Thus for $\omega_e\tau_R<1$, $W_e^{SR}\gg W_e^{G}$, since the bracketed term in Eq. (18) should be of order of magnitude unity. While for $\omega_e\tau_R>1$ (which is usually the case at reduced temperatures in X-band experiments) $W_e^{G}$ and $W_e^{SR}$ are of comparable order of magnitude and they both depend inversely on $\tau_R$. Thus from Eq. (17) we may define an essentially temperature-independent quantity $A$ such that:

$$W_e\equiv AT/\eta. \quad (19)$$

TABLE VI. Reduction factor, $R$, for unsaturated observing transition.[a,b]

| Line pumped | Line observed: +1 | 0 | −1 |
|---|---|---|---|
| +1 | ··· | $(b+b^2)/(1+3b+b^2)$ | $b^2/(1+3b+b^2)$ |
| 0 | $b/(1+b)$ | ··· | $b/(1+b'')$ |
| −1 | $b^2/(1+3b+b^2)$ | $(b+b^2)/(1+3b+b^2)$ | ··· |

[a] See Eq. (9).
[b] The table gives the results for END only. For exchange only, replace all nonzero elements in the table by $b''/(1+b'')$.

[19] We have used the fact that $\Sigma_i(g_i^2-g_e^2)=\Sigma_i(g_i-g_e)^2$ which follows from $\Sigma_i(g_i-g_e)=0$.

TABLE VII. Reduction factor, $R$, for strongly saturated observing transition.[a,b]

| Line pumped | Line observed: +1 | 0 | −1 |
|---|---|---|---|
| +1 | ... | $b/(1+3b)$ | $b^2/(1+3b+2b^2)$ |
| 0 | $(b+2b^2)/(1+4b+3b^2)$ | ... | $(b+2b^2)/(1+4b+3b^2)$ |
| −1 | $b^2/(1+3b+2b^2)$ | $b/(1+3b)$ | ... |

[a] See Eq. (10).
[b] The table gives the results for END only. For exchange only, replace all nonzero elements in the table by $b''/(1+2b'')$.

The dependence of $W_n^{\mathrm{END}}$ on $\tau_R$ is quite different:[11,12,15]

$$W_n^{\mathrm{END}}=\tfrac{1}{10}\gamma_e^2\gamma_n^2\hbar^2\sum_m (D_n^{(m)}D_n^{(-m)})\tau_R, \quad (20)$$

where $\gamma_n$ is the nuclear magnetogyric factor, and the $D_n^{(m)}$ are the anisotropic dipolar terms discussed in Ref. 15. In Eq. (20), one uses the fact that $\omega_n\tau_R\ll 1$ in liquids so that

$$W_n^{\mathrm{END}}\equiv B\eta/T. \quad (20')$$

Thus,

$$b=(B/A)(\eta/T)^2 \quad (21)$$

so that $b$ should increase significantly with decreasing $T$.

Most studies on Heisenberg exchange are consistent with a strong exchange for which[20–22]

$$\omega_{\mathrm{HE}}=16\pi Da[R], \quad (22)$$

where $D$ is the translational diffusion coefficient given in a Stokes–Einstein model by

$$D=kT/6\pi a\eta, \quad (23)$$

and $[R]$ is the radical concentration in molecules per cubic centimeter. Thus we define

$$\omega_{\mathrm{HE}}\equiv 6C[R]T/\eta \quad (22')$$

so that

$$b''=(C/A)[R] \quad (24)$$

which is temperature independent. Unlike Heisenberg exchange, chemical exchange is usually not diffusion controlled so that its temperature dependence is generally different from that of $D$, although its rate also increases with increasing temperature.[23]

## V. DISCUSSION

There is general agreement between the results of the experiments described in Sec. III and the theory of Sec. IV. Thus:

(1) The observed EPR line is *reduced* in intensity (or indirectly saturated) by the application of the pump microwave power (Figs. 8 and 9).

(2) At low temperatures and concentrations, the reduction decreases (i.e., the effect diminishes) as the number of hyperfine intervals separating the observing and pumping microwave frequencies is increased. In addition, as the temperature of dilute samples is increased, the reduction decreases. These observations are consistent with a dominant electron-nuclear dipole (END) mechanism which causes relatively rapid nuclear relaxations (Fig. 10).

(3) At higher temperatures and concentrations the reduction becomes independent of the number of hyperfine separations and independent of the temperature. It is dependent, under these conditions, on concentration. This is consistent with a Heisenberg exchange (HE) mechanism (Fig. 10).

(4) The reduction asymptotically reaches a maximum value as the pumping power is increased, and this is true under conditions when the END mechanism dominates and also when the HE mechanism dominates (Figs. 12 and 13).

(5) When the observing microwave power is increased to a level where it begins to saturate the observed line, the reduction effect is diminished (Fig. 11).

The experiments reported here were designed primarily to obtain the basic effect and to demonstrate its salient features. The experimental values of $R$ in the tables and in Fig. 10 were determined for the most part under conditions which yielded best signal-to-noise ratios. For the nitroxide radical, which is moderately difficult to saturate, both the observing and pumping microwave powers usually were at partial saturation

[20] G. E. Pake and T. R. Tuttle, Jr., Phys. Rev. Letters **3**, 423 (1959); D. Kivelson, J. Chem. Phys. **27**, 1094 (1960); J. D. Currin, Phys. Rev. **126**, 1995 (1962); J. H. Freed, J. Chem. Phys. **45**, 3452 (1966); C. S. Johnson, Jr., Mol. Phys. **12**, 25 (1967).

[21] For weaker exchange one obtains:

$$\omega_{\mathrm{HE}}=\omega_{\mathrm{HE}}^{\max}(J\tau_d)^2(1+J^2\tau_d^2)^{-1},$$

where $\tau_d$ is the lifetime of the collision pair and $J$ is the exchange integral, cf. Ref. 20.

[22] There is some discrepancy in Refs. 12 and 20 with regard to the numerical factor in Eq. 22. The factor of 16 employed here is based upon the derivation by S. Chandrasekhar, Rev. Mod. Phys. **15**, 1 (1943), for the rate at which particles describing Brownian motion will coalesce: $4\pi D_{ik}r_{ik}[R]^2$. The relative diffusion $D_{ik}=2D$, where $D$ is the normal diffusion rate for a single particle, and $r_{ik}$ the distance the radicals must approach to interact is taken as a minimum of $2a$. Experimental values for $\omega_{\mathrm{HE}}$ appear to be closer to half the magnitude predicted by Eq. 22.

[23] R. L. Ward and S. I. Weissman, J. Am. Chem. Soc. **79**, 2086 (1957); C. S. Johnson, Jr., Advan. Magnetic Resonance **1**, 89 (1965).

levels. Thus it is difficult to extract precise values for the relaxation times based on the theory of Sec. IV. It is clear that asymptotic values of $R$ could be determined in the manner of Figs. 12 and 13 for each of the entries in the tables and in Fig. 10. This useful but tedious program has, however, been deferred to the future.

Nevertheless, it seems appropriate to attempt the exercise of extracting numerical values from the experiments which have been performed. A study of Table I and the saturation curves of Figs. 6 and 7 suggest that the best data for determining $b$ are when pumping on the center interval and observing the low-field +1 line. Both of these transitions are fairly well saturated, indicating that Table VII should be used, and the fact that neither is completely saturated gives rise to errors which tend to cancel. One obtains values of $b=1$, 0.39 and 0.14 for $T=-80°$, $-50°$, and $-20°$C. It is apparent from Fig. 10 that the reductions at +10°C (Table I.D) arise from a mixture of END and HE mechanisms, and no effort has been made to utilize the data at this temperature. From Eq. (21), a plot of $b$ versus $(\eta/T)^2$ should yield a straight line. Using the viscosity data for ethylbenzene (4.79, 2.24, and 1.245 cP at $-80°$, $-50°$, and $-20°$C),[24] one does in fact obtain a reasonable straight line through these three points.

If we assume that the longitudinal relaxation process is dominated by $g$-tensor and spin–rotational mechanisms, then an expression for $b$ as a function of the isotropic rotational correlation time $\tau_R$ can be derived. Our experimental values of $b$ then permit a determination of $\tau_R$. This calculation is based on the work of McConnell and his colleagues,[25] who have studied a number of nitroxide radicals that are closely related to I and have measured their anisotropic parameters. They have found that the dipolar and $g$ tensors are nearly constant for these radicals and suggest using dipolar parameters which, in the present notation, are[26] $\zeta_n D_N^0 \approx 30$ MHz and $D_N^m \approx 0$ for $m \neq 0$, where $\zeta_n = (1/2\pi)\gamma_e\gamma_N\hbar$. The $g$ tensor is approximated by their accurately determined values for di-*tertiary*-butyl nitroxide (DTBN):[25,27] $g_x=2.0089$; $g_y=2.0061$; $g_z=2.0027$.

Using these numerical values we have from Eqs. (15), (16), and (20):

$$W_e^{SR} \approx 3.23\times10^{-6}\tau_R^{-1}\ \text{sec}^{-1}, \tag{25a}$$

$$W_e^{G} \approx 0.475\times10^{-6}[\omega_e^2\tau_R/(1+\omega_e^2\tau_R^2)]\ \text{sec}^{-1}, \tag{25b}$$

and

$$W_N^{END} \approx 3.55\times10^{15}\tau_R\ \text{sec}^{-1}. \tag{26}$$

We assume for simplicity that $\omega_e\tau_R>1$ (although this does not appear quite to be the case, see below) so that:

$$W_e \approx 3.7\times10^{-6}\tau_R^{-1}\ \text{sec}^{-1} \tag{25c}$$

and

$$b \approx 9.6\times10^{20}\tau_R^2. \tag{27}$$

Thus we obtain $\tau_R \approx 3.2$, 2.0 and $1.2\times10^{-11}$ sec for $b=1$, 0.39, and 0.14, respectively.

No attempt has been made to demonstrate unequivocally that $W_e$ is just $W_e^{SR}+W_e^{G}$ in these systems. Although the work of Plachy and Kivelson[28] lends some support to this, the small correlation times suggest that the END terms should be making appreciable contributions to $W_e$ as well as to cross transitions.[11]

An alternative approach is to determine $W_e$ experimentally. There are numerous experimental and theoretical difficulties in obtaining the longitudinal relaxation time from an inhomogeneously broadened line, but various order of magnitude attempts using the data of Fig. 7 suggest that $W_e$ is somewhat greater than predicted by Eq. (25c) using these values of $\tau_R$.

Once a value of $\tau_R$ has been obtained, Eq. (17) can be used to calculate an effective molecular radius. The effective radius has been estimated by Maki *et al.*[27] for DTBN in methylcyclohexane, $a=0.9$ Å, and by Plachy and Kivelson[28] for DTBN in $n$-pentane, $a=1.8$ Å. These values are much less than actual molecular dimensions. For nitrobenzene-anion radicals in polar solvents, correlation times are about an order of magnitude greater and correspond to values of "$a$" which are comparable to the actual molecular dimensions.[29] Using the theoretical estimate for $W_e$ above, a value is obtained for the nitroxide radical I in ethylbenzene of 1.9 Å. No very great significance should be placed on this result, but it would appear that more refined experiments of the type suggested by the present work could yield useful numbers.

The electron–electron double resonance experiments on Coppinger's radical demonstrate that $W_H^{END}$ must be much smaller than $W_N^{END}$. This is to be expected, since the anisotropic dipolar interaction of protons is

[24] "Selected Values of Properties of Hydrocarbons and Related Compounds," American Petroleum Institute, Research Project 44, 1955, Table 21c–K (Part I), p. 1.

[25] (a) O. H. Griffith, D. W. Cornell, and H. M. McConnell, J. Chem. Phys. **43**, 2909 (1965); (b) T. J. Stone, T. Buckman, P. L Nordio, and H. M. McConnell, Proc. Natl. Acad. Sci. U.S. **54**, 1010 (1965).

[26] McConnell *et al.*[25] explicitly give $|A| \approx 87$ MHz and $|B| = |C| \approx 14$ MHz in the principal axis system. In the present notation $\zeta_N D_N^0 = (6^{\frac{1}{2}}/4)[A-a]$ and $\zeta_N D_N^{\pm2} = (1/4)[B-C]$ with $\zeta_N D_N^{\pm1}=0$, where $a=(1/3)(A+B+C)$. It might be noted in this context that the best available estimate of $\zeta_N D_N^0$ for one unpaired electron in the nitrogen $2p\pi$ orbital is 58.5 MHz. [A. Horsfield, J. R. Morton, J. R. Rowlands, and D. H. Whiffen, Mol. Phys. **5**, 241 (1962) and J. R. Morton, J. R. Rowlands, and D. H. Whiffen, National Physical Laboratory, Teddington, England, Bulletin No. BPR 13, 1962.] Thus these nitroxide radicals appear to have a $2p$–$\pi$-nitrogen spin density of 0.5 rather than the value of $\approx 0.9$ suggested by McConnell *et al.*

[27] N. A. Edelstein, A. Kwok, and A. H. Maki, J. Chem. Phys. **41**, 179 (1964).

[28] W. Plachy and D. Kivelson, J. Chem. Phys. **47**, 3312 (1967). We wish to thank these authors for communication of this work prior to publication.

[29] J. H. Freed, J. Chem. Phys. **41**, 2077 (1964).

with electron-spin density on *adjacent* carbon atoms, whereas the $^{14}N$ nucleus interacts with its own $2p$–$\pi$ unpaired electron density and the magnitude of $\langle r^{-3}\rangle$ is much greater. Typically, $W_H^{END}$ is about an order of magnitude smaller than $W_N^{END}$.[11]

The result that the reductions when Heisenberg exchange dominates are substantially greater for Coppinger's radical than for the nitroxide radical under similar conditions of solvent viscosity, temperature, and concentration follows immediately from the difference in $W_e$ for the two compounds. Even for comparable exchange rates, $b'$ (or $b''$) will be greater for Coppinger's radical and the reduction, $R$, will be greater. The experimental difficulty in achieving a satisfactory level of microwave-power saturation of the nitroxide radical under those conditions where Heisenberg exchange dominates will decrease the observed nitroxide reductions still further.

If values of $W_e$ were known, the present experiments in the HE region would yield exchange frequencies and thus be a direct check on the validity of Eqs. (22) and (23). If the data on Coppinger's radical is processed by utilizing Eq. (13), values of $b'=2.22$, 0.64, and 0.25 are obtained for $3\times10^{-4}$, $10^{-4}$, and $3\times10^{-5}M$ solutions. These values of $b''$ have the expected linear dependence on concentration. For the nitroxide radical, however, values of $b''=0.25$, 0.087 and 0.031 for $10^{-2}$, $10^{-3}$, and $3\times10^{-4}M$ were measured. These represent a significant departure from linearity with respect to concentration which probably is associated with increasing microwave-power saturation difficulties as the concentration becomes higher.

One interesting approach to the interpretation of these experiments is to assume that Eqs. (22) and (23) are valid (which appears to be a reasonably sound assumption based on experimental measurements on DTBN in a variety of solvents)[28,30,31] and that the value of $b''$ found at lowest concentration of the nitroxide radical, where the sample is most strongly saturated by the pump power, is correct. We then obtain a value for $W_e$ which can be extrapolated to lower temperatures assuming an $\eta/T$ dependence. This value can be used in conjunction with the measurement of $b$ to determine $\tau_R$ and the effective radius $a$. Following this procedure using the relationship $W_e=\omega_{EX}/6b''$, we obtain for the constant $A$ in Eq. (19)

$$A=4[R]k/9b'', \tag{28}$$

and from Eqs. (17) and (26),

$$a=\left[\left(\frac{kT}{\eta}\right)^2\frac{b[R]}{3\pi b''3.55\times10^{15}}\right]^{1/3}=3.8\text{ Å}. \tag{29}$$

If the factor of 2 mentioned in Ref. 22 is introduced empirically, we get $a=3.0$ Å.

[30] T. A. Miller, R. N. Adams, and P. M. Richards, J. Chem. Phys. **44**, 4022 (1966).
[31] M. Eastman and J. H. Freed (unpublished results).

By means of the experimental and theoretical approaches given here, ratios of $W_n/W_e$ and $\omega_{HE}/W_e$ are obtained as functions of temperature. If any one of the three quantities $W_n$, $\omega_{HE}$ or $W_e$ is known at a particular temperature from an independent experiment or theoretical model, the other two can be found for all temperatures, and if two of the quantities are assumed known, then we have a check for internal consistency of the models and experimental techniques.

It is obvious, as one considers the present experiments, that sweeping the magnetic field is a much less preferable technique than sweeping one of the microwave frequencies. It is felt that a cavity of the type used here, Figs. 1 and 2, will be appropriate for frequency sweeps. A variety of experimental difficulties can be anticipated, but there is little doubt but that a microwave-frequency-swept electron–electron double resonance spectrometer can be built.

One of the applications of such a device is that it could be possible to obtain the $T_i$'s in systems such as the nitroxide radical I, where the hyperfine lines are each inhomogeneously broadened. Thus, assuming the inhomogeneous line is an envelope of several narrow Lorentzians, it should be possible to saturate preferentially one such component without significantly affecting the others. By sweeping the observing microwave frequency (assumed to be nonsaturating) through another inhomogeneously broadened hyperfine interval, a difference signal would be detected only for that Lorentzian component of the observing transition which corresponds (in terms of local field) to the one being saturated. That is, from Eq. (5)

$$(Z_{EPR}''-Z_{DEPR}'')\propto\frac{\xi_{o,i}}{\Omega_{p,o}{}^i}\left(\frac{T_{o,i}}{1+\Delta\omega_{o,i}{}^2T_{o,i}{}^2}\right), \tag{30}$$

where $\xi_{o,i}$ given by Eq. (6) is adjusted to have significant magnitude only for the $i$th component of the pumped line. The width of the difference signal given by Eq. (30) is just $T_{o,i}{}^{-1}$.

It would also be possible to sweep the pumping frequency while keeping $\Delta\omega_{o,c}=0$, but the line shape obtained would be that of a saturated Lorentzian. Experimentally it would seem that a sweep of the pumping microwave source is preferable, since any noise introduced because of automatic frequency-control tracking difficulties would not reach the observing microwave detector crystal. It may be that a plot of the observed linewidth versus microwave pump power in an experiment where the pump frequency is swept can be extrapolated to give reliable values for $T_{o,i}{}^{-1}$.

The same technique outlined in the previous few paragraphs should be useful for the analytical purpose of determining hyperfine couplings in complex spectra. For example, in radicals with both nitrogen and proton couplings of comparable magnitude, the greater values of $W_N^{END}$ for the nitrogen nuclei may permit precise determination of the nitrogen couplings.

## VI. SUMMARY

It is our impression that electron–electron double resonance is a somewhat neglected technique, probably because of the experimental difficulties associated with the bimodal cavity. It is obvious from the present work that there are many possibilities for the study of systems in the liquid phase using these methods. In addition to the experiments described here, we have examined in a rather cursory manner a large number of unrelated systems in crystalline, glass, and liquid phases—more or less going through the samples which happen to be at hand. Signals were detected in nearly all cases. Our summary statement is that it would appear that the technique of electron–electron double resonance has wide applicability in chemical physics.

## ACKNOWLEDGMENT

Professor H. M. McConnell gave us considerable encouragement during the course of this work and participated in several helpful discussions.

THE JOURNAL OF CHEMICAL PHYSICS VOLUME 48, NUMBER 9 1 MAY 1968

# Energy Dependence of Charge-Transfer Reactions in the Thermal and Low-Electron-Volt Region*

FRED A. WOLF† AND B. R. TURNER

*Gulf General Atomic Incorporated, John Jay Hopkins Laboratory for Pure and Applied Science, San Diego, California*

(Received 6 November 1967)

A method is presented for extrapolating to lower energies the cross sections for charge transfer which have been measured by beam techniques for incident kinetic energies greater than 1 eV. The method combines the Rapp and Francis resonance charge-transfer theory with the Langevin capture model, and is based upon a simple superposition of the "noncapture resonance" and "capture resonance" probabilities resulting in charge transfer. Also illustrated is a method for including nonrectilinear orbits in the Rapp and Francis model. Application of the theory to the negative-ion charge-transfer reactions $O^-$, $O_2^-$, $O_3^-$, and $OH^-$ with $NO_2$; the positive-ion charge-transfer reactions $O^+$, $O_2^+$, $N^+$, and $N_2^+$ with NO; and $N^+$ with $O_2$ is given, and comparisons with existing experimental data are made. The method appears to be a reasonable approximation provided that the relative probability of the charge-transfer channel emerging from the capture-formed complex is independent of the relative kinetic energy of the reactants.

## I. INTRODUCTION

Atomic and molecular beams have been a major experimental tool for obtaining data relevant to collisions of ions and neutrals. A beam of ions may be directed into a static gas, or an ion beam and a beam of neutral particles may be made to intersect in a small interaction region not immediately surrounded by surfaces. Very accurate control can be achieved over both the reactants and products with the latter method. The use of ion beams is, however, generally limited to incident ion energies greater than about 1 eV.

For many applications to aeronomy, plasma physics, radiation chemistry, and in the study of processes in flames, discharges, and shock tubes, data are needed for interaction energies in the range between 1 eV and thermal energy (0.03 to 0.1 eV). While there are several techniques for measuring many of the desired quantities at thermal energies, it is difficult to extend the results of these measurements to higher collision energies. Hence, it is useful to extrapolate to lower collision energies the results obtained in the energy region above 1 eV by beam techniques.

In previous theoretical studies, two energy regions, "low" and "intermediate," have been considered separately. In the low-energy region the strong attraction between the ion and neutral which arises, due to the charge-induced dipole interaction between the constituents, is dominant. In this region Langevin-type capture orbitals occur and, good estimates for reaction cross sections are frequently obtained by using the maximum impact parameter for capture. In the intermediate-energy range, where the charge-induced dipole interaction is less important, resonant charge-transfer theories have been based upon rectilinear paths for the colliding particles.

In this paper, a method is presented for combining these two models so that it becomes possible to obtain the energy dependence of cross sections for resonant charge transfer continuously over both energy regions. It is not claimed that data will always fit this model, since neither the low-energy nor the intermediate-energy theories comprising the model always hold; but since both the underlying models have found widespread use it is useful to unify these theories. The

* Research sponsored by the Defense Atomic Support Agency under Contract DA-49-146-XZ-354.

† Permanent address: San Diego State College, San Diego, Calif.